

Property Comparison of Thermoplastic Starch Reinforced by Cellulose Nanofibrils with Different Chemical Compositions

Chan-Woo Park,^a Song-Yi Han,^a Pureun-Narae Seo,^a Won-Jae Youe,^{a,b} Yong Sik Kim,^a Seon-Kang Choi,^c Nam-Hun Kim,^a and Seung-Hwan Lee^{a,*}

Masterbatch composites made from starch/glycerol mixtures having 50 parts per hundred resin (phr) of three cellulose nanofibrils (CNFs) with different chemical compositions were prepared by pre-gelatinizing starch to create better dispersion of CNFs. The CNF contents were adjusted to 1, 5, 10, and 30 phr by adding ungelatinized starch and glycerol to the obtained masterbatch composite. The composite was then extruded at 150 °C using a twin-screw extruder. The average diameters of the lignocellulose nanofibrils (LCNF), holocellulose nanofibrils (HCNF), and pure cellulose nanofibrils (PCNF) were 53.1, 24.4, and 22.4 nm, respectively. By increasing the CNF content in all nanocomposites, the tensile strength and elastic modulus were improved, whereas the elongation at break was diminished. Tensile properties were higher in the order of thermoplastic starch (TPS)/HCNF > TPS/PCNF > TPS/LCNF nanocomposites when the same CNF content was used. The addition of LCNF and PCNF also improved the thermal and moisture stability, whereas a negative effect was found in the TPS/HCNF nanocomposite. The effect of the LCNF on the thermal and water stability was greater than that of the HCNF and PCNF composites. The water uptake of the TPS/HCNF nanocomposite was higher than that of the TPS without CNFs.

Keywords: Thermoplastic starch; Lignocellulose nanofibril; Holocellulose nanofibril; Twin-screw extrusion; Nanocomposite

Contact information: a: College of Forest and Environmental Science, Kangwon National University, Chun-Cheon 200-701, Republic of Korea; b: Division of Wood Chemistry, National Institute of Forest Science, Seoul, 02455, Republic of Korea; c: Department of Agricultural Life Industry, Kangwon National University, Chun-Cheon 200-701, Republic of Korea; *Corresponding author: lshykh@kangwon.ac.kr

INTRODUCTION

In recent years, environmental pollution caused by petroleum-derived plastic wastes has worsened. As an alternative to petroleum-derived plastics, bio-based plastics based on natural polymers such as starch, cellulose, lignin, and protein have attracted attention (Chang *et al.* 2010; Liu *et al.* 2010; Girones *et al.* 2012; Cobut *et al.* 2014; Balakrishnan *et al.* 2017; Drakopoulos *et al.* 2017). Specifically, starch is a highly advantageous material for bio-based plastics because of its low cost, biodegradability, biocompatibility, and high applicability (Karimi *et al.* 2014; Müller *et al.* 2014; Khan *et al.* 2017). Also, it is one of the most abundant biopolymers in nature, mostly found in corn, potato, rice, fruit, and other plants. It is a homopolymer of α -D-glucose, which consists of amylose and amylopectin with semi-crystallinity (Li and Huneault 2011; Mendes *et al.* 2016). Starch can be gelatinized in the presence of plasticizers, such as water, glycerol, and sorbitol (Martins *et al.* 2009; Ghanbari *et al.* 2018). Upon heating (90 to 180 °C) and

mechanical shearing, the structure and crystallinity of starch granules can be disrupted due to the starch-plasticizer interaction (Carmona *et al.* 2015; González *et al.* 2015). Thermoplastic starch (TPS) is the most widely used bioplastic and has a high annual growth rate.

However, TPS has some drawbacks, such as a low water resistance and low mechanical properties, which limits its range of application (Belhassen *et al.* 2014; Karimi *et al.* 2014; Müller *et al.* 2014; Balakrishnan *et al.* 2017). Various reinforcing fillers, such as montmorillonite, clay, carbon nanotube, and cellulosic fiber, can be used to improve the properties of TPS (Huang *et al.* 2004; Dean *et al.* 2007; Martins *et al.* 2009). Recently, natural cellulosic fiber, especially nanocellulose, has gained attention as a reinforcing filler for TPS (Hietala *et al.* 2013; Nasri-Nasrabadi *et al.* 2014; González *et al.* 2015; Drakopoulos *et al.* 2017; Kargarzadeh *et al.* 2017; Ghanbari *et al.* 2018; Fazeli *et al.* 2018; Fazeli *et al.* 2019).

Nanocellulose can be prepared from lignocellulosic biomass by mechanical fibrillation or hydrolysis. Because the nanocellulose has beneficial properties, such as high strength (10 GPa), elastic modulus (130 to 140 GPa), large specific surface area, and high thermal stability (Samir *et al.* 2005; Eichhorn *et al.* 2010; Lee *et al.* 2010; Balakrishnan *et al.* 2017), it can greatly enhance various properties of TPS (Hietala *et al.* 2013; Nasri-Nasrabadi *et al.* 2014). Hietala *et al.* (2013) prepared TPS/cellulose nanofibril (CNF) composites from a mixture of potato starch/sorbitol/stearic acid/CNF by twin-screw extrusion between 80 and 110 °C; the tensile properties of the TPS/CNF composite were improved as the CNF content increased. Furthermore, the addition of CNF reduced the moisture sensitivity, which is one of the largest disadvantages of TPS composites. The moisture diffusion coefficient and moisture equilibrium content also decreased with increasing CNF content.

Previous research (Park *et al.* 2017a,b) has focused on the characterization and application of lignocellulose nanofibrils (LCNF) containing both lignin and hemicellulose, and holocellulose nanofibrils (HCNF) with a high hemicellulose content without lignin. The properties of CNF and its reinforced composites can be controlled by adjusting the chemical composition. The hydrophobic lignin on the surface of LCNF improves the thermoflowability, water stability, and mechanical properties, but lowers the dispersibility in hydrophilic polymers. HCNF has a core-shell structure in which the hemicellulose covers the cellulose core and has a high potential as a reinforcing filler for hydrophilic polymers (Galland *et al.* 2015; Park *et al.* 2017a, b). Hemicellulose can act as an adhesive between the nanofibril and the hydrophilic matrix polymer because of its strong hydrophilic properties, thereby improving the strength and hardness of the composites.

In this study, three types of CNFs with different chemical compositions, *i.e.*, LCNF, HCNF, and pure cellulose nanofibril (PCNF), were used as the reinforcing fillers for TPS. The effects of the chemical composition and content of these CNFs on the mechanical properties, thermal properties, and water stability of the CNF-reinforced TPS composites were compared.

EXPERIMENTAL

Materials

For the CNF preparation, yellow poplar (*Liriodendron tulipifera* L.), which consists of 45.4% cellulose, 26.3% hemicellulose, and 28.3% lignin (Park *et al.* 2017b), was

obtained from the Experimental Forest of Kangwon National University (Chuncheon, Republic of Korea). Corn starch, glycerol, sodium chlorite, acetic acid, sodium hydroxide, and tert-butyl alcohol were purchased from Daejung Chemicals & Metals Co., Ltd. (Siheung, Republic of Korea) and used without further purification.

Delignification and alkaline treatment

Delignification to obtain holocellulose was conducted according to the following process. Wood powder (20 g) was added into distilled water (1,200 mL) and kept in a water bath at 80 °C while being stirred at 150 rpm. The delignification reaction was initiated by adding sodium chlorite (8 g) and acetic acid (1,600 µL) to the suspension. The reactant was continuously stirred for 1 h. The same amount of sodium chlorite and acetic acid was added every hour, and the process was repeated 7 times. The obtained residue, namely holocellulose, was purified by vacuum-filtration with distilled water. The pure cellulose was prepared from the obtained holocellulose through successive alkaline treatment. The holocellulose (30 g) was poured into a 17.5% sodium hydroxide solution (750 mL). The reaction was performed for 50 min while being stirred at 150 rpm at a temperature between 20 and 23 °C. At the end of the reaction time, 10% acetic acid (750 mL) was added to the solution for neutralization. The reactant was vacuum-filtrated and washed with distilled water.

Methods

Preparation of CNFs

The wood powder for LCNF preparation was suspended in water to obtain a concentration of 5.0 wt.% (3,000 mL), and holocellulose and pure cellulose for HCNF and PCNF preparation were suspended to obtain a concentration of 1.0 wt.% (1,500 mL). The suspensions were subjected to wet disk milling (WDM) (Supermasscolloider, MKCA6-2, Masuko Sangyo Co. Ltd., Kawaguchi, Japan). The rotational speed was set to 1800 rpm, and the clearance between the upper and lower disks was reduced to between 80 and 150 µm from the zero point, at which the disks would begin to rub.

The operation for LCNF was repeated until the 15th pass was completed, and the operations for HCNF and PCNF were repeated until the 5th pass. The duration was recorded for each number of WDM passes, and each WDM time (h/kg) was calculated based on the solid weight.

Preparation of TPS/CNF composites

First, masterbatch composites with a high content of CNFs (50 phr based on starch and glycerol weight) were prepared according to the following method. Starch and glycerol were mixed to obtain a 75/25 ratio, respectively, and added into the CNF suspensions in water (1.5 wt. %).

Gelatinization was performed at 85 °C for 90 min with a stirring speed of 150 rpm, and then the mixtures were dried on polytetrafluoroethylene (PTFE) sheets in an oven dryer at 60 °C for 24 h. Next, the mixture of the ungelatinized starch/glycerol (75/25) was added into the masterbatch composite to dilute the CNF content from 50 phr to 1, 5, 10, and 30 phr, consecutively (Table 1). Then, the mixtures were extruded using a twin-screw extruder (BA-11, Bautek Co., Ltd., Pochen, Republic of Korea) with a 40 length/diameter (*L/D*) ratio at 150 °C with a rotational speed of 100 rpm.

Table 1. Material Formulation for TPS/CNF Composites

Sample Code	Starch/Glycerol (75/25) Mixture (g)	TPS/CNF Masterbatch Composite		Total (g)
		Starch/glycerol (75/25) (g)	CNFs (g)	
TPS	100	-	-	100
TPS with 1 phr CNF	98	2	1	101
TPS with 5 phr CNF	90	10	5	105
TPS with 10 phr CNF	80	20	10	110
TPS with 30 phr CNF	40	60	30	130

Morphological observation

The CNF samples for the scanning electron microscope (SEM) observation were prepared according to the following method. The LCNF, HCNF, and PCNF suspensions were diluted to 0.001 wt.% and sonicated using an ultrasonicator (VCX130PB, Sonics & Materials Inc., Newtown, CT, USA) for 1 min. The suspensions were vacuum-filtrated on a PTFE membrane filter. The filtrated products, which were stacked on the PTFE filter, were immersed in tert-butyl alcohol for 30 min. This immersion procedure was repeated three times to completely exchange the water with the tert-butyl alcohol. The CNFs were freeze-dried using a freeze dryer (FDB-5502, Operon Co. Ltd., Gimpo, Republic of Korea) at -55 °C for 3 h to prevent the aggregation of CNFs.

The freeze-dried CNF samples and fractured TPS/CNF nanocomposites were then coated with iridium using a high-vacuum sputter coater (EM ACE600, Leica Microsystems, Ltd., Wetzlar, Germany). The coating thickness was approximately 2 nm. The morphologies of the CNFs and TPS were observed using a SEM (S-4800, Hitachi Co. Ltd, Tokyo, Japan) in the Central Laboratory at Kangwon National University. The diameter of individual fibers was measured at least 400 times on each sample by ImageJ software (National Institute of Health, U.S.A.)

Thermogravimetric (TG) analysis

TG analysis of the TPS/CNF nanocomposites was conducted using a TG analyzer (Q2000, TA Instruments Inc., New Castle, DE, USA) in the Central Laboratory of Kangwon National University. The samples (5 to 10 mg) were heated on a platinum pan under a nitrogen atmosphere. The range of the scanning temperature was from 25 to 500 °C, with a heating rate of 10 °C/min. The derivative TG (DTG) analysis was conducted by measuring mass loss with respect to temperature.

Tensile properties

TPS/CNF nanocomposites were hot-pressed at 150 °C for 1 min for sheet formation. For tensile testing, the specimens were prepared from the sheet according to Type V dimensions described by the American Society for Testing and Materials D638 standard and were kept in a thermos-hygrostat (SJ-109, SoJung Measuring Instrument Company Co. Ltd., Anyang, Republic of Korea) at 25 °C and 65% relative humidity (RH) to standardize the effect of RH on the tensile properties. The tensile test was conducted using a tensile testing machine (H50K, Hounsfield Test Equipment, Redhill, UK) with a cross-head speed of 10 mm/min. At least 9 specimens of each sample were tested, and the average values were taken.

Water uptake

TPS/CNF nanocomposite sheets prepared by hot-pressing at 150 °C were cut to dimensions of 10 x 10 mm with a 2 mm thickness. The specimens were air-dried at 80 °C for 12 h and vacuum-dried at 40 °C until the weight of the composites was constant. Then, the samples were conditioned at 25 ± 2 °C with 43, 59, 75, and 98% RH, consecutively. The RH was adjusted using saturated solutions of potassium carbonate, sodium bromide, sodium chloride, and potassium sulfate, respectively. The weight of the samples was measured until it was constant, and the water uptake (W_U) was calculated by the following equation,

$$W_U(\%) = \frac{M_c - M_0}{M_0} \times 100 \quad (1)$$

where M_0 is the initial weight and M_c is the constant weight of humid specimens.

RESULTS AND DISCUSSION

Morphological Characteristics of LCNF, HCNF, and PCNF

The morphological characteristics of the LCNF, HCNF, and PCNF prepared at similar WDM times of 6 to 7 h/kg are shown in Fig. 1. In the LCNF, incompletely defibrillated fibrils of 100 nm thickness, which were covered with lignin-like particles, were present alongside 20 nm thick fibers, while the HCNF and PCNF had uniform fiber morphologies with a diameter of 20 to 35 nm. The average diameters of the LCNF, HCNF, and PCNF were 53.1 ± 24.1, 24.4 ± 9.2, and 22.4 ± 8.4 nm, respectively. Although three types of CNFs were defibrillated at similar WDM times, the diameter was larger in the order of LCNF > HCNF > PCNF. This phenomenon was due to the improvement in defibrillation efficiency resulting from the removal of lignin and hemicellulose. Because the existence of lignin and hemicellulose disturbs the defibrillation of cellulose microfibrils, narrower fibers with a uniform morphology can be obtained after chemical pretreatment for the removal of lignin and hemicellulose, especially lignin.

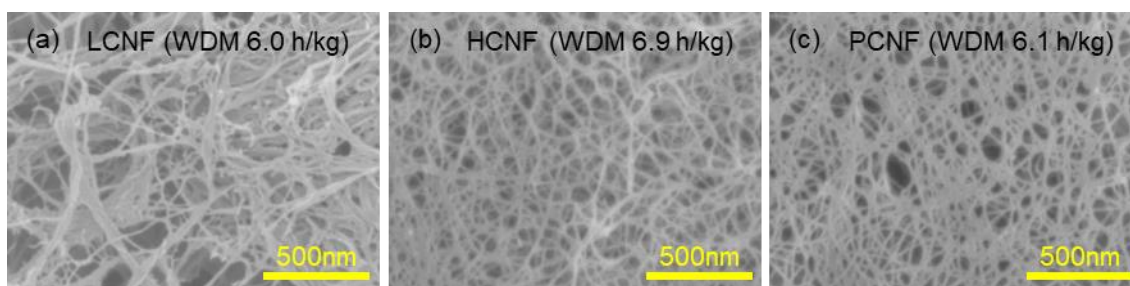


Fig. 1. Morphological characterization of (a) lignocellulose nanofibril (LCNF), (b) holocellulose nanofibril (HCNF), and (c) pure cellulose nanofibril (PCNF)

Properties of TPS/CNF Masterbatch Composite

To enhance the dispersity of CNFs in the TPS matrix, starch was pre-gelatinized in the presence of glycerol and CNF suspensions of water, which resulted in a masterbatch composite with a 50 phr CNF content. Figure 2 shows the morphological characteristics of the fractured surface of the neat TPS and TPS/CNF masterbatch composite. The neat TPS without CNFs had a smooth fractured surface with a hyphae-like pattern, which may have been due to the recrystallization of starch (Wang *et al.* 2012). On the other hand, the

masterbatch composite had a rough fractured surface that showed both aggregated and individual CNFs. The difference in dispersity among the CNFs with different chemical compositions was not significant.

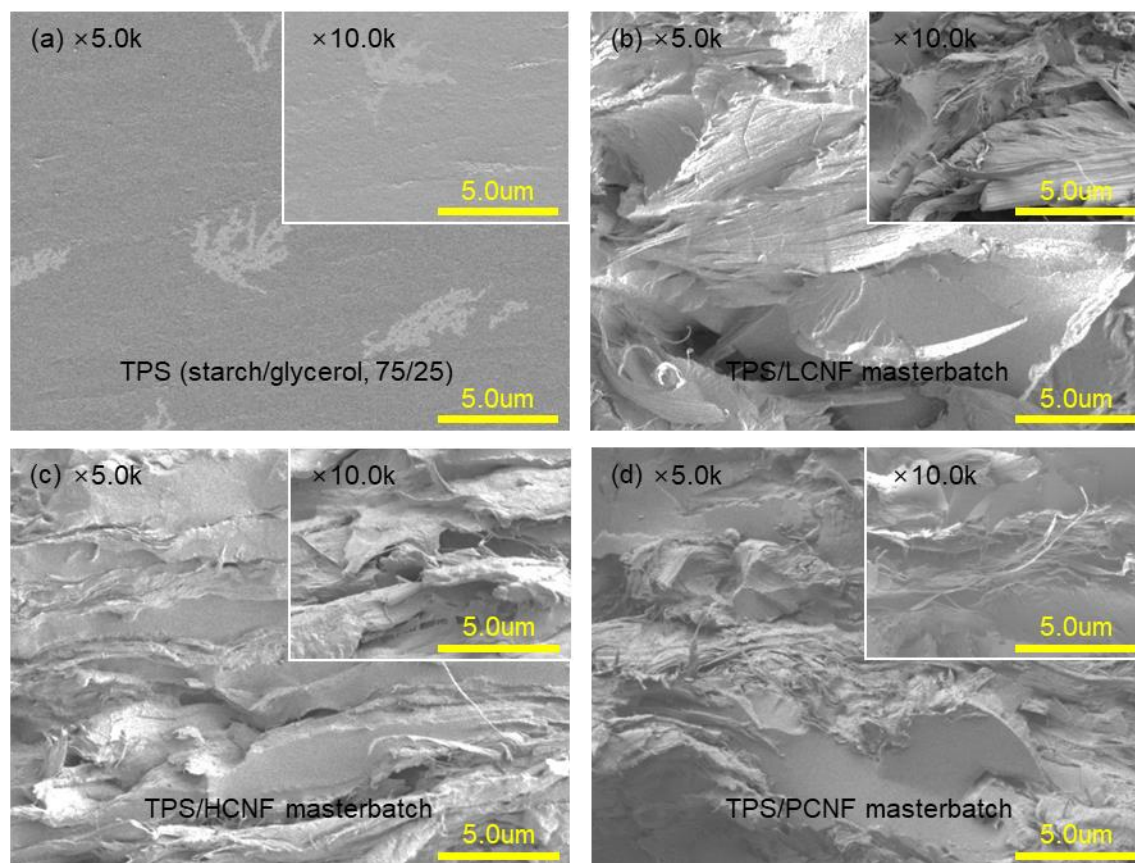


Fig. 2. Morphological characterization of thermoplastic starch (TPS)/cellulose nanofibril (CNF) masterbatch composites with 50 phr in (a) Neat TPS without CNFs, (b) TPS/lignocellulose nanofibril (LCNF), (c) TPS/holocellulose nanofibril (HCNF), and (d) TPS/pure cellulose nanofibril (PCNF) masterbatch composites

Figure 3 indicates the effect of the addition of CNFs with different chemical compositions on tensile strength, elastic modulus, and elongation at break of the TPS/CNF masterbatch composites. The addition of all CNFs improved the tensile strength and elastic modulus, which were higher in the order of TPS/HCNF > TPS/PCNF > TPS/LCNF masterbatch composites. Because the tensile properties of the TPS may have been influenced by the hydrogen bonding between starch molecules, the hydrophilicity of the LCNF, HCNF, and PCNF, dependent on their chemical composition, was an important factor for the tensile properties of the masterbatch composite. In previous studies (Kim *et al.* 2017; Park *et al.* 2017a,b), the tensile strength and elastic modulus of nanopapers obtained from LCNF, HCNF, and PCNF were higher in the order of HCNF > PCNF > LCNF, thereby showing a similar tendency with the tensile properties of the TPS/CNF masterbatch composite. Because of the hydrophobicity of the lignin on the surface of LCNF, the nanopaper from the LCNF had a lower tensile strength and elastic modulus than those of the HCNF and PCNF, which was attributed to a lack of hydrogen bonding between the cellulose molecules. In the case of HCNF with a core-shell structure, hemicellulose is present on the surface of cellulose and may act as an adhesive between the cellulose fibrils

to improve tensile properties (Galland *et al.* 2015; Prakobna *et al.* 2016). This characteristic of HCNF could have contributed to the improvement in tensile properties of TPS. The elongation at break of TPS was 11.5%, which decreased to less than 3% with CNF addition.

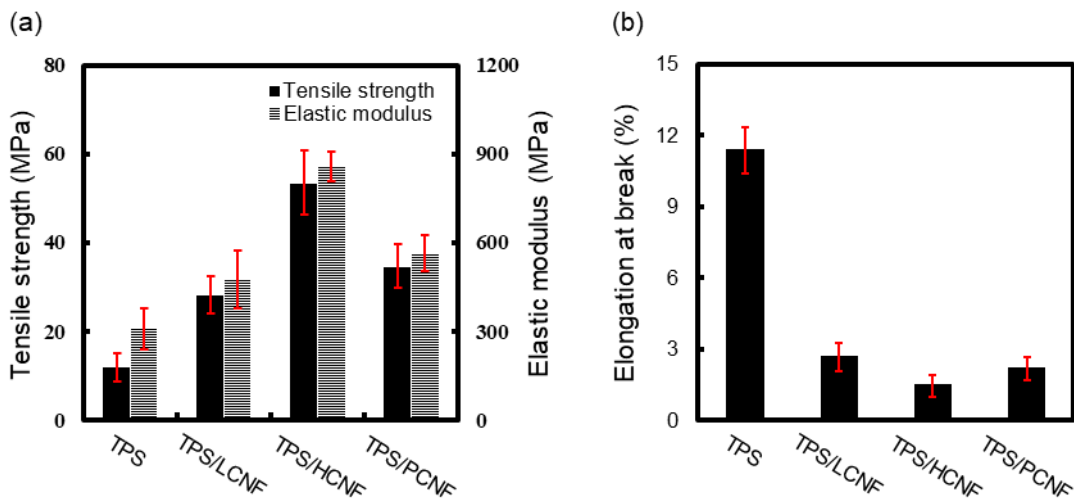


Fig. 3. (a) Tensile strength, elastic modulus, and (b) elongation at break of thermoplastic starch (TPS)/cellulose nanofibril (CNF) masterbatch composites with lignocellulose nanofibril (LCNF), holocellulose nanofibril (HCNF), and pure cellulose nanofibril (PCNF) contents of 50 phr

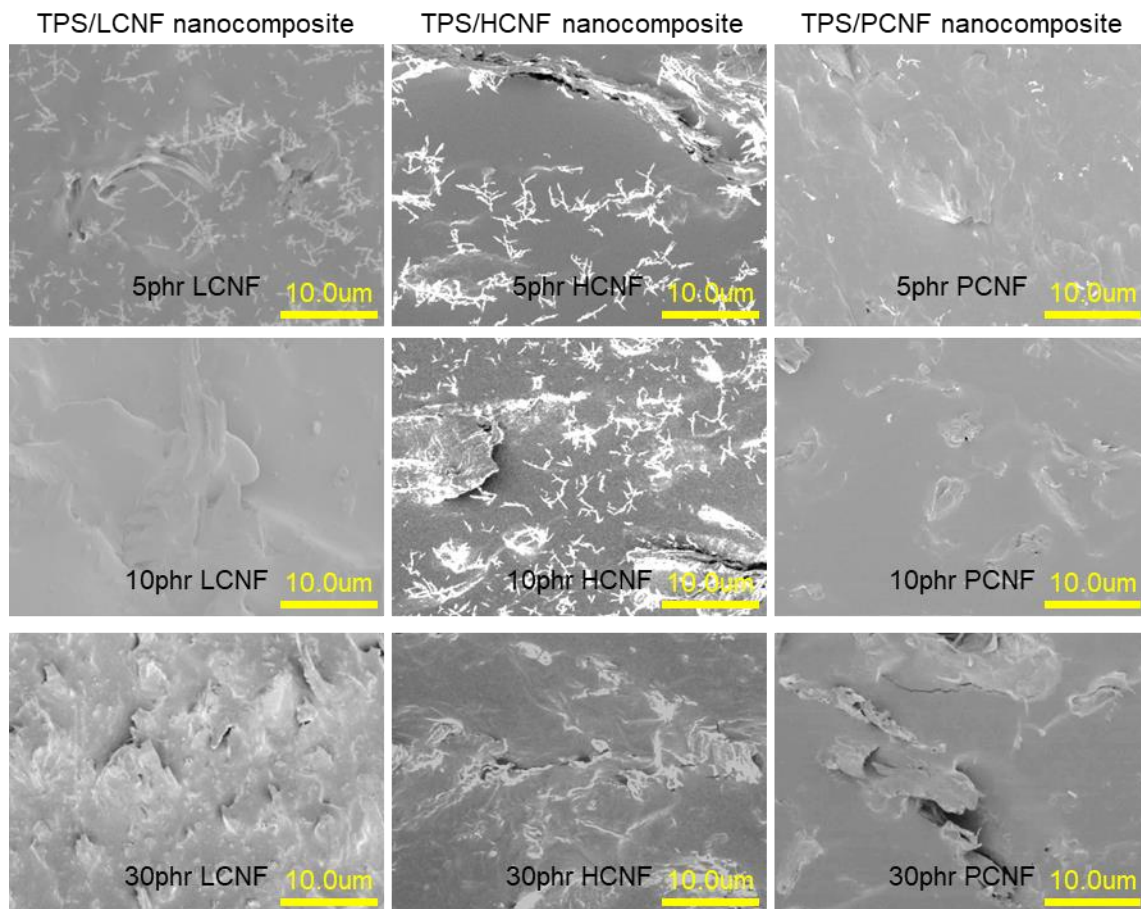


Fig. 4. Morphological characterization of thermoplastic starch (TPS)/cellulose nanofibril (CNF) nanocomposites with different contents of CNFs

Properties of TPS/CNF Nanocomposite

Figure 4 shows the morphological characteristics of the TPS/CNF nanocomposites with different CNF contents, which were prepared from the TPS/CNF masterbatch composite by adding additional starch and glycerol. The nanocomposites also showed that the hyphae-like pattern shown in the masterbatch composite was due to recrystallization of starch and particles formed by the aggregation of CNFs. As the content of CNFs increased, the fractured surface of the nanocomposites tended to be rough and showed a decreasing dispersity of CNFs in the TPS matrix.

The effect of the CNF content and chemical composition on the tensile properties of the TPS/CNF nanocomposites is shown in Fig. 5. The TPS in Fig. 3 was prepared by plasticizing starch with glycerol and water to create better dispersion of CNFs in the matrix for the preparation of the masterbatch composite. However, the TPS in Fig. 5 was plasticized by using extrusion in the presence of glycerol without water. The tensile strength and elastic modulus of the TPS, which are shown in Fig. 3, were higher than those of the TPS, which is shown in Fig. 5, and the elongation at break was lower. This phenomenon could be explained by anti-plasticization (Chang *et al.* 2006; Sreekumar *et al.* 2013). In the plasticization process of starch by glycerol, the glycerol penetrates the starch granules, thereby creating intermolecular spaces between the starch molecules and reducing the intermolecular interaction. This results in an increase in flexibility, thereby lowering the tensile strength. However, in the case of plasticization in the presence of both glycerol and water, the regeneration possibility of intermolecular hydrogen bonding between starch molecules increases after the evaporation of water. This anti-plasticization effect can improve the tensile properties of TPS. Chang *et al.* (2006) reported the tensile properties of TPS prepared from starch/water suspensions of 2 wt. % with different glycerol contents. As the glycerol content was increased from 0 to 20%, based on the weight of the starch, the tensile strength of the TPS decreased gradually. It was stated that this result was due to the anti-plasticizing effect of water on the tensile strength of TPS. All TPS/CNF composites had a higher tensile strength and elastic modulus than the TPS without CNFs and showed a lower elongation at break than that of the TPS. In all TPS/CNF nanocomposites, the tensile strength and Young's modulus improved with increasing CNF content, whereas the elongation at break decreased. The reinforcing effect of LCNF in TPS composites was inferior to that of the other samples because of the hydrophobic property of lignin on the surface of the CNFs. The tensile properties of the TPS/HCNF nanocomposites were significantly improved by increasing the HCNF content. In Fig. 3, the results showed similar tendencies with the TPS/CNF masterbatch composite, which were mainly related to the difference in hydrophilicity of the CNFs.

The TG and DTG curves of TPS without CNFs and the TPS/CNF nanocomposites with LCNF, HCNF, and PCNF (30 phr) are shown in Fig. 6. All samples began to decompose rapidly at temperatures in the range of 280 to 330 °C, and two noticeable peaks were observed in the DTG curves. The initial peak at 280 °C corresponded to the decomposition of glycerol in the TPS matrix. The main peak, of which the maximum point was located at 312 °C, was attributed to by the thermal degradation of starch. Unlike TPS, the peak due to the decomposition of glycerol at 280 °C was reduced in the TPS/CNF composites.

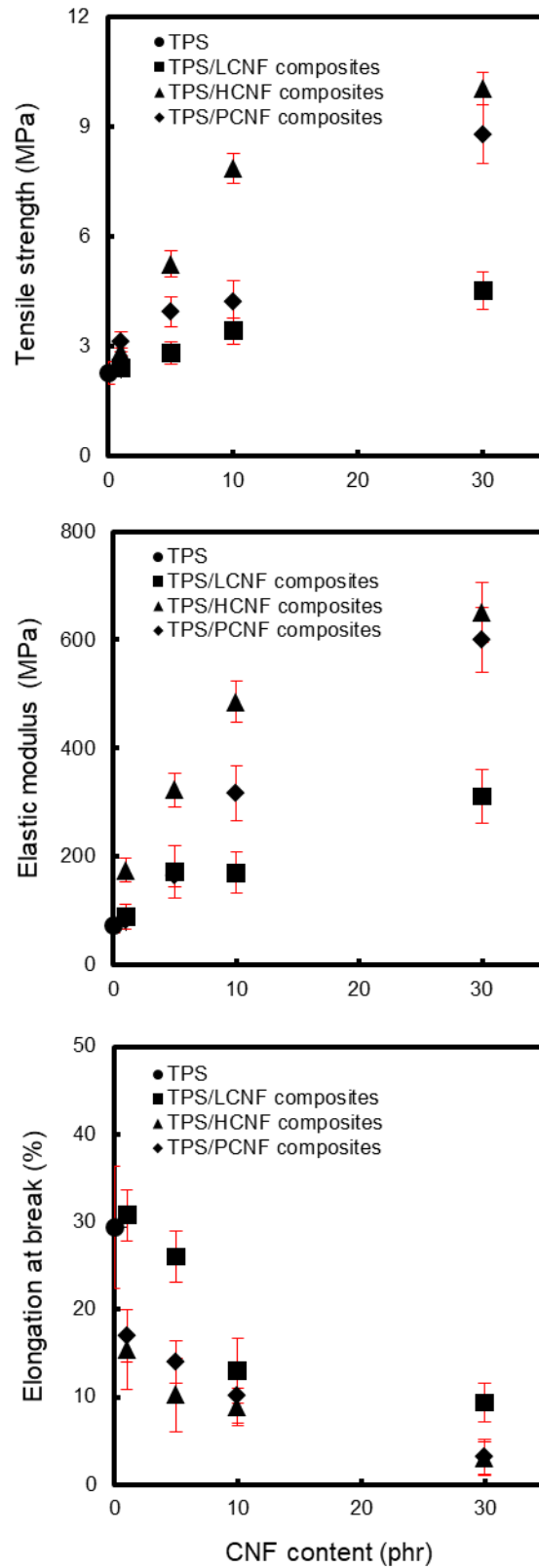


Fig. 5. Tensile strength, elastic modulus, and elongation at break of thermoplastic starch (TPS)/cellulose nanofibril (CNF) nanocomposites with different CNF contents

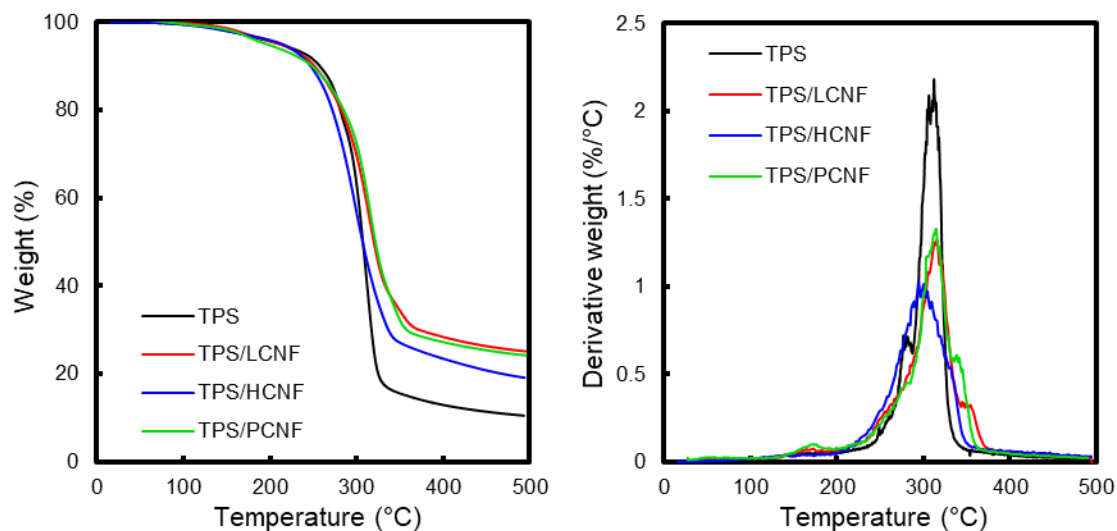


Fig. 6. Thermogravimetric and derivative thermogravimetric curves of thermoplastic starch (TPS)/cellulose nanofibril (CNF) nanocomposites with lignocellulose nanofibril (LCNF), holocellulose nanofibril (HCNF), and pure cellulose nanofibril (PCNF) contents of 30 phr

In the TPS/LCNF and PCNF nanocomposites, the thermal degradation temperature was higher than that of the TPS, but the TPS/HCNF composite began to decompose at a lower temperature than the other samples. This may have been due to the high content of hemicellulose and no lignin content in the HCNF. Because the molecular weight of hemicellulose is lower than that of cellulose and lignin, the hemicellulose that surrounds the cellulose core in HCNF is vulnerable to heat (Agustin-Salazar *et al.* 2018). The effect of HCNF content on the thermal properties of the TPS/HCNF composite is shown in Fig. 7. As the HCNF content increased, the amount of residue increased. In addition, the temperature at which the thermal decomposition started to decrease, and the maximum point of the main peak shifted toward a lower temperature. These results proved that the HCNF addition reduced the temperature at which the decomposition started due to high hemicellulose content.

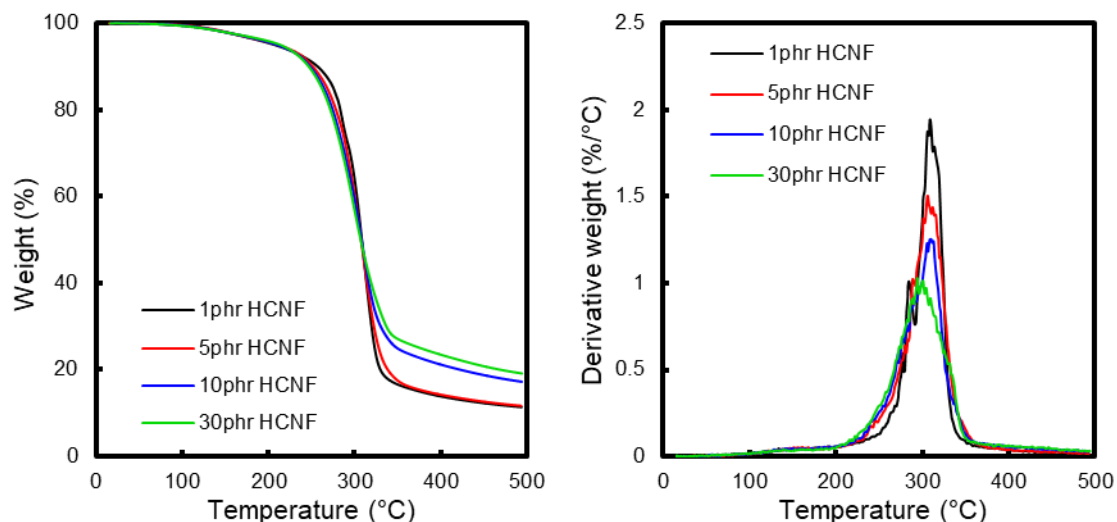


Fig. 7. Thermogravimetric and derivative thermogravimetric curves of thermoplastic starch (TPS)/holocellulose nanofibril (HCNF) nanocomposites with different HCNF contents

Table 2. Water Uptake of TPS/CNF Nanocomposites with Different CNF Contents

	CNF Content (phr)	Water Uptake in Equilibrium (%)			
		43 RH	59 RH	75 RH	98 RH
TPS	-	7.3 ± 0.6	11.0 ± 0.2	22.5 ± 0.7	80.7 ± 2.0
TPS/LCNF	1	7.0 ± 0.5	11.0 ± 0.8	19.9 ± 0.6	78.6 ± 1.4
	5	6.0 ± 0.8	10.6 ± 0.2	19.8 ± 0.4	69.3 ± 1.4
	10	5.7 ± 0.6	9.4 ± 0.5	18.6 ± 0.4	67.1 ± 1.6
	30	5.4 ± 0.6	8.7 ± 0.9	19.9 ± 0.2	61.0 ± 1.0
TPS/HCNF	1	8.1 ± 0.8	12.2 ± 0.6	24.0 ± 0.3	89.2 ± 1.2
	5	8.2 ± 0.9	12.4 ± 0.8	22.4 ± 0.8	85.7 ± 3.4
	10	7.9 ± 0.8	11.5 ± 0.9	21.5 ± 0.7	84.2 ± 2.0
	30	7.5 ± 0.7	11.1 ± 0.4	21.6 ± 0.6	83.0 ± 1.2
TPS/PCNF	1	7.2 ± 0.5	11.1 ± 0.9	21.2 ± 1.0	78.5 ± 0.3
	5	7.0 ± 0.8	10.8 ± 0.5	20.8 ± 0.5	73.5 ± 2.4
	10	6.1 ± 0.6	10.7 ± 0.4	19.3 ± 0.4	69.5 ± 3.4
	30	5.8 ± 0.4	9.4 ± 0.3	18.4 ± 0.5	66.2 ± 1.4

Table 2 shows the water uptake of TPS/CNF nanocomposites with different CNF contents in equilibrium at 43, 59, 75, and 98% RH. In all samples, as the RH increased, the water uptake of the TPS and TPS/CNF nanocomposites also increased and showed the maximum water uptake to be at 98% RH. Due to the addition of LCNF and PCNF, the water uptake was lower than that of TPS without CNFs and decreased gradually with increasing CNF content. It is well known that TPS is very sensitive to moisture. Many studies have reported that the addition of cellulosic fiber, including CNF, is one of the most effective ways to reduce the moisture absorption of TPS (Karimi *et al.* 2014; Ghanbari *et al.* 2018). Karimi *et al.* (2014) reported that because of CNF addition, the water uptake of starch composites prepared with 33.3 wt. % glycerol at 98% RH decreased from values above 65% to below 50% with increasing CNF content. Fazeli *et al.* (2018) also reported that the water vapor transmission rate (WVTR) of the starch composite film gelatinized by glycerol was reduced as a result of the CNF addition. In Table 2, the TPS/LCNF nanocomposites had the lowest water uptake at all RH conditions. The hydrophobic lignin contained in LCNF may interrupt water absorption by the TPS/LCNF nanocomposites. On the other hand, the water uptake of the TPS/HCNF nanocomposites was higher than that of the TPS without CNFs, which may have been due to the strong hygroscopic characteristics of HCNF. Moreover, the decrease in water uptake with increasing HCNF content was not significant compared to other nanocomposites.

CONCLUSIONS

1. Thermoplastic starch (TPS) nanocomposites labeled as TPS/LCNF, HCNF, and PCNF nanocomposites were prepared by twin-screw extrusion from TPS/CNF masterbatch composites with 50 phr of lignocellulose nanofibrils (LCNF), holocellulose nanofibrils (HCNF), and pure cellulose nanofibrils (PCNF) for better dispersion of CNFs in TPS.
2. The effects of different chemical compositions of CNFs and their content on the properties of TPS/CNF nanocomposites were investigated. In all nanocomposites, the tensile strength and elastic modulus improved with an increasing content of CNFs, whereas the elongation at break decreased.

3. The tensile strength and elastic modulus of TPS/CNF masterbatch composites and nanocomposites were higher in the order of TPS/HCNF > TPS/PCNF > TPS/LCNF, which may have been due to the different hydrophilicity of the CNFs.
4. The thermal and moisture stability were also affected by different chemical compositions and amounts of CNFs. In the TPS/LCNF and PCNF composites, the thermal degradation temperature was higher than that of the TPS, whereas the TPS/HCNF nanocomposite started to decompose at a lower temperature than other samples, which was due to the poor thermal resistance of HCNF.
5. The water uptake of TPS/LCNF and PCNF nanocomposites decreased at all RH conditions with an increasing CNF content, whereas the TPS/HCNF nanocomposite showed higher water uptake than that of the TPS and other nanocomposites due to strong hydrophilicity of HCNF.

ACKNOWLEDGMENTS

This research was supported by the Basic Science Research Program through the National Research Foundation of Korea (NRF) funded by the Ministry of Education (No. 2015R1D1A1A01061522 and 2018R1A6A1A03025582). The authors thank Dr. Sun-Young Lee at the National Institute of Forest Science in the Republic of Korea for measuring the tensile strength of the specimens.

REFERENCES CITED

- Agustin-Salazar, S., Cerruti, P., Medina-Juárez, L.Á., Scarinzi, G., Malinconico, M., Soto-Valdez, H., and Gamez-Meza, N. (2018). "Lignin and holocellulose from pecan nutshell as reinforcing fillers in poly(lactic acid) biocomposites," *International Journal of Biological Macromolecules* 115, 727-736. DOI: 10.1016/j.ijbiomac.2018.04.120
- Balakrishnan, P., Sreekala, M. S., Kunaver, M., Huskić, M., and Thomas, S. (2017). "Morphology, transport characteristics and viscoelastic polymer chain confinement in nanocomposites based on thermoplastic potato starch and cellulose nanofibers from pineapple leaf," *Carbohydrate Polymers* 169, 176-188. DOI: 10.1016/j.carbpol.2017.04.017
- Belhassen, R., Vilaseca, F., Mutjé, P., and Boufi, S. (2014). "Thermoplasticized starch modified by reactive blending with epoxidized soybean oil," *Industrial Crops and Products* 53, 261-267. DOI: 10.1016/j.indcrop.2013.12.039
- Carmona, V. B., Corrêa, A. C., Marconcini, J. M., and Mattoso, L. H. C. (2015). "Properties of a biodegradable ternary blend of thermoplastic starch (TPS), poly (ϵ -caprolactone) (PCL) and poly (lactic acid) (PLA)," *Journal of Polymers and the Environment* 23(1), 83-89. DOI: 10.1007/s10924-014-0666-7
- Chang, P. R., Jian, R., Zheng, P., Yu, J., and Ma, X. (2010). "Preparation and properties of glycerol plasticized-starch (GPS)/cellulose nanoparticle (CN) composites," *Carbohydrate Polymers* 79(2), 301-305. DOI: 10.1016/j.carbpol.2009.08.007
- Chang, Y. P., Karim, A. A., and Seow, C. C. (2006). "Interactive plasticizing-

- antiplasticizing effects of water and glycerol on the tensile properties of tapioca starch films,” *Food Hydrocolloids* 20(1), 1-8. DOI: 10.1016/j.foodhyd.2005.02.004
- Cobut, A., Sehaqui, H., and Berglund, L. A. (2014). “Cellulose nanocomposites by melt compounding of TEMPO-treated wood fibers in thermoplastic starch matrix,” *BioResources* 9(2), 3276-3289. DOI: 10.15376/biores.9.2.3276-3289
- Dean, K., Yu, L., and Wu, D. Y. (2007). “Preparation and characterization of melt-extruded thermoplastic starch/clay nanocomposites,” *Composites Science and Technology* 67(3-4), 413-421. DOI: 10.1016/j.compscitech.2006.09.003
- Drakopoulos, S. X., Karger-Kocsis, J., Kmetty, A., Lendvai, L., and Psarras, G. C. (2017). “Thermoplastic starch modified with microfibrillated cellulose and natural rubber latex: A broadband dielectric spectroscopy study,” *Carbohydrate Polymers* 157, 711-718. DOI: 10.1016/j.carbpol.2016.10.036
- Eichhorn, S. J., Dufresne, A., Aranguren, M., Marcovich, N. E., Capadona, J. R., Rowan, S. J., Weder, C., Thielemans, W., Roman, M., Renneckar, S., and Gindl, W. (2010). “Current international research into cellulose nanofibres and nanocomposites,” *Journal of Materials Science* 45(1), 1. DOI: 10.1007/s10853-009-3874-0
- Fazeli, M., Keley, M., and Biazar, E. (2018). “Preparation and characterization of starch-based composite films reinforced by cellulose nanofibers,” *International Journal of Biological macromolecules* 116, 272-280. DOI: 10.1016/j.ijbiomac.2018.04.186
- Fazeli, M., Florez, J. P., and Simão, R. A. (2019). “Improvement in adhesion of cellulose fibers to the thermoplastic starch matrix by plasma treatment modification,” *Composites Part B: Engineering* 163, 207-216. DOI: 10.1016/j.compositesb.2018.11.048
- Galland, S., Berthold, F., Prakobna, K., and Berglund, L. A. (2015). “Holocellulose nanofibers of high molar mass and small diameter for high-strength nanopaper,” *Biomacromolecules* 16(8), 2427-2435. DOI: 10.1021/acs.biomac.5b00678
- Ghanbari, A., Tabarsa, T., Ashori, A., Shakeri, A., and Mashkour, M. (2018). “Preparation and characterization of thermoplastic starch and cellulose nanofibers as green nanocomposites: Extrusion processing,” *International Journal of Biological Macromolecules* 112, 442-447. DOI: 10.1016/j.ijbiomac.2018.02.007
- Girones, J., Lopez, J. P., Mutje, P., Carvalho, A. J. F. D., Curvelo, A. A. D. S., and Vilaseca, F. (2012). “Natural fiber-reinforced thermoplastic starch composites obtained by melt processing,” *Composites Science and Technology* 72(7), 858-863. DOI: 10.1016/j.compscitech.2012.02.019
- González, K., Retegi, A., González, A., Eceiza, A., and Gabilondo, N. (2015). “Starch and cellulose nanocrystals together into thermoplastic starch bionanocomposites,” *Carbohydrate Polymers* 117, 83-90. DOI: 10.1016/j.carbpol.2014.09.055
- Hietala, M., Mathew, A. P., and Oksman, K. (2013). “Bionanocomposites of thermoplastic starch and cellulose nanofibers manufactured using twin-screw extrusion,” *European Polymer Journal* 49(4), 950-956. DOI: 10.1016/j.eurpolymj.2012.10.016
- Huang, M. F., Yu, J. G., and Ma, X. F. (2004). “Studies on the properties of montmorillonite-reinforced thermoplastic starch composites,” *Polymer* 45(20), 7017-7023. DOI: 10.1016/j.polymer.2004.07.068
- Kargarzadeh, H., Johar, N., and Ahmad, I. (2017). “Starch biocomposite film reinforced by multiscale rice husk fiber,” *Composites Science and Technology* 151, 147-155.

- DOI: 10.1016/j.compscitech.2017.08.018
- Karimi, S., Dufresne, A., Tahir, P. M., Karimi, A., and Abdulkhani, A. (2014). "Biodegradable starch-based composites: Effect of micro and nanoreinforcements on composite properties," *Journal of Materials Science* 49(13), 4513-4521. DOI: 10.1007/s10853-014-8151-1
- Khan, B., Bilal Khan Niazi, M., Samin, G., and Jahan, Z. (2017). "Thermoplastic starch: A possible biodegradable food packaging material - A review," *Journal of Food Process Engineering* 40(3), e12447. DOI: 10.1111/jfpe.12447
- Kim, B. Y., Han, S. Y., Park, C. W., Chae, H. M., and Lee, S. H. (2017). "Preparation and properties of cellulose nanofiber films with various chemical compositions impregnated by ultraviolet-curable resin," *BioResources* 12(1), 1767-1778. DOI: 10.15376/biores.12.1.1767-1778
- Lee, S. H., Chang, F., Inoue, S., and Endo, T. (2010). "Increase in enzyme accessibility by generation of nanospace in cell wall supramolecular structure," *Bioresource Technology* 101(19), 7218-7223. DOI: 10.1016/j.biortech.2010.04.069
- Li, H., and Huneault, M. A. (2011). "Comparison of sorbitol and glycerol as plasticizers for thermoplastic starch in TPS/PLA blends," *Journal of Applied Polymer Science* 119(4), 2439-2448. DOI: 10.1002/app.32956
- Liu, D., Zhong, T., Chang, P. R., Li, K., and Wu, Q. (2010). "Starch composites reinforced by bamboo cellulosic crystals," *Bioresource Technology* 101(7), 2529-2536. DOI: 10.1016/j.biortech.2009.11.058
- Martins, I. M., Magina, S. P., Oliveira, L., Freire, C. S., Silvestre, A. J., Neto, C. P., and Gandini, A. (2009). "New biocomposites based on thermoplastic starch and bacterial cellulose," *Composites Science and Technology* 69(13), 2163-2168. DOI: 10.1016/j.compscitech.2009.05.012
- Mendes, J. F., Paschoalin, R. T., Carmona, V. B., Neto, A. R. S., Marques, A. C. P., Marconcini, J. M., Mattoso, L. H. C., Medeiros, E. S., and Oliveira, J. E. (2016). "Biodegradable polymer blends based on corn starch and thermoplastic chitosan processed by extrusion," *Carbohydrate Polymers* 137, 452-458. DOI: 10.1016/j.carbpol.2015.10.093
- Müller, P., Renner, K., Móczó, J., Fekete, E., and Pukánszky, B. (2014). "Thermoplastic starch/wood composites: Interfacial interactions and functional properties," *Carbohydrate Polymers* 102, 821-829. DOI: 10.1016/j.carbpol.2013.10.083
- Nasri-Nasrabadi, B., Behzad, T., and Bagheri, R. (2014). "Preparation and characterization of cellulose nanofiber reinforced thermoplastic starch composites," *Fibers and Polymers* 15(2), 347-354. DOI: 10.1007/s12221-014-0347-0
- Park, C. W., Han, S. Y., Choi, S. K., and Lee, S. H. (2017a). "Preparation and properties of holocellulose nanofibrils with different hemicellulose content," *BioResources* 12(3), 6298-6308. DOI: 10.15376/biores.12.3.6298-6308
- Park, C. W., Han, S. Y., Namgung, H. W., Seo, P. N., Lee, S. Y., and Lee, S. H. (2017b). "Preparation and characterization of cellulose nanofibrils with varying chemical compositions," *BioResources* 12(3), 5031-5044. DOI: 10.15376/biores.12.3.5031-5044
- Prakobna, K., Berthold, F., Medina, L., and Berglund, L. A. (2016). "Mechanical performance and architecture of biocomposite honeycombs and foams from core-shell holocellulose nanofibers," *Composites Part A: Applied Science and Manufacturing* 88, 116-122. DOI: 10.1016/j.compositesa.2016.05.023
- Samir, M. A. S. A., Alloin, F., and Dufresne, A. (2005). "Review of recent research into

- cellulosic whiskers, their properties and their application in nanocomposite field,” *Biomacromolecules* 6(2), 612-626. DOI: 10.1021/bm0493685
- Sreekumar, P. A., Leblane, N., and Saiter, J. M. (2013). “Effect of glycerol on the properties of 100 % biodegradable thermoplastic based on wheat flour,” *Journal of Polymers and the Environment* 21(2), 388-394. DOI: 10.1007/s10924-012-0497-3
- Wang, S. J., Blazek, J., Gilbert, E. P., and Copeland, L. (2012). “New insights on the mechanism of acid degradation of pea starch,” *Carbohydrate Polymers* 87, 1941-1949. DOI: 10.1016/j.carbpol.2011.09.093

Article submitted: November 3, 2018; Peer review completed: January 1, 2019; Revised version received: January 2, 2019; Accepted: January 3, 2019; Published: January 10, 2019.

DOI: 10.15376/biores.14.1.1564-1578